RZ 2993 (# 93039) 02/23/98
Engineering & Technology 13 pages

Research Report

On the Molecular Beam Deposition of Organic Light-Emitting Devices

Samuel Strite* and Eliav I. Haskal

IBM Research Division
Zurich Research Laboratory
8803 Rüschlikon
Switzerland

*Present address: Uniphase Laser Enterprise, Zürich, Switzerland

On the Molecular Beam Deposition of Organic Light-Emitting Devices

Samuel Strite* and Eliav I. Haskal

IBM Research Division, Zurich Research Laboratory, 8803 Rüschlikon, Switzerland

Abstract

We describe the conversion of a commercial molecular beam epitaxy system from GaAs epitaxy to organic molecular beam deposition (OMBD). Our optimized procedures developed over several years of OMBD operation are also described.

*Present address: Uniphase Laser Enterprise, Zürich, Switzerland

I. INTRODUCTION

In 1987, Tang and VanSlyke[1] demonstrated efficient organic electroluminescence (EL) in a multilayer device vacuum-deposited on a simple indium-tin-oxide (ITO) coated glass substrate. Since then, numerous groups have begun to investigate organic light-emitting devices (OLEDs) because of their promising potential for inexpensively fabricated displays.[2] Tang and VanSlyke used a stand-alone bell jar thermal evaporator to fabricate their devices, and most investigators have followed their example. However, as development progresses, research is moving away from simple, discrete OLEDs towards more complicated device and display architectures. Therefore more sophisticated vacuum deposition systems having increased source capacity, improved cleanliness, greater reproducibility and control as well as the flexibility of vacuum interconnectivity with additional process tools are becoming desirable.

At the same time, inorganic compound semiconductor technology has advanced rapidly while new materials whose economic potential remains unexploited have decreased. Today's cutting-edge optoelectronic research relies more heavily on device fabrication and system design than on innovative epitaxial techniques. The traditional lone molecular beam epitaxy (MBE) practitioner is thus finding it more difficult to perform innovative small-scale compound semiconductor device research. In addition, optoelectronic device production is increasingly being performed using the higher throughput metalorganic chemical vapor deposition (MOCVD) technique. The preference for MOCVD production has already idled MBE systems in various corporate laboratories, and this trend can be expected to spill over into universities. Given the large number of GaAs-type MBE machines in both university and industrial laboratories, it is likely that numerous MBE systems will be redirected towards the deposition of alternative materials, including organic compounds.

This paper describes the conversion of a GaAs MBE to an organic molecular beam deposition (OMBD) system. It also describes our operating procedures developed over several years of OMBD experience and serves as a road map to other researchers working in the OLED field who may wish to convert a commercial MBE system.

II. MBE DESCRIPTION

The MBE system was originally used for eight years as a conventional solid-source crystal growth system for the production of InAlGaAs semiconductor laser diodes.[3] It was manufactured by Intevac using the Varian Gen II design. Figure 1 is a current photograph of the OMBD system at IBM's Zurich research laboratory.

The OMBD incorporates a source flange containing eight effusion cell ports, four of which are tilted upwards and four downwards. Three of these ports and the effusion cells mounted therein are visible in the left-hand side of Fig. 1. A mass spectrometer is attached to the chamber in the center of the photo and its cables connect it to the box just above it. Just behind the box is a vacuum feedthrough that controls a main shutter. By rotating the feedthrough, the shutter can be moved in front of the sample like a pendulum. The main shutter is used for crude shadow masking and to shield the substrate from source flux, which leaks around the individual effusion cell shutters. On the far side of the chamber, a quartz crystal monitor mounted on a stepper-motor-controlled feedthrough can be identified by the two black quartz crystal coolant hoses arching down and back up. The motor permits the quartz monitor to be positioned within the molecular beams directly in front of the substrate for flux measurement, and retracted during sample growth.

The OMBD chamber is pumped continuously by an ion pump and a cryopump. A titanium sublimation pump is also available and is used for accelerating pumpdown from atmosphere.

The MBE system is designed to be modular, meaning that an arbitrary number of additional chambers can be vacuum-connected with a common transfer system. Typically, GaAs researchers connect either a surface analysis chamber or a second MBE to increase the number of materials that can be explored in single structures. Instead, we added an rf-plasma processing chamber, which we use for ITO/glass substrate cleaning in an oxygen plasma.[4] We have also equipped this rf-plasma chamber with a substrate heater and two effusion cells, which, along with the gases that can be introduced through the rf-plasma source or through a separately controlled leak valve, provide us with a wide range of process and deposition possibilities to complement the OMBD.

Figure 2 is a photograph showing the greater interconnected vacuum system comprising the OMBD chamber, the rf-plasma processing chamber, and the vacuum load lock and transfer chamber. The turbopumped rf-plasma chamber can be seen behind the OMBD to the right of center of the photo. To the right of the plasma chamber is the cryopumped load lock for sample introduction. In the foreground is the ion-pumped transfer chamber, which acts as a vacuum buffer between the load lock and OMBD. Two magnets are seen resting on top of the transfer chamber. These magnets are used to guide the sample holder cassette along rails between the load lock and transfer chamber. Extending from the right of the load lock and transfer chambers are magnetically coupled transfer arms, which permit samples to be removed from the cassette and inserted into the plasma chamber or OMBD, respectively.

Figure 3 is a schematic of the OMBD interior. The sample manipulator accommodates circular substrate holders with a 3" diameter and can be rotated at variable speed during deposition to improve sample uniformity. An ion flux gauge is mounted on the reverse side of the sample holder to enable direct measurement of source-material beam-equivalent pressures. The water-cooled substrate heater is capable of heating a substrate to at least 800 °C. The entire source and sample area is surrounded by a cryoshroud designed to condense background gas in the chamber to improve cleanliness in the deposition zone. Reflection high-energy electron diffraction (RHEED) and mass spectrometry are used for *in situ* analysis of crystal growth and quantification of background gas concentrations.

A typical GaAs MBE system contains Ga, Al, In, As, Si, and Be sources, which have evaporation temperatures between 500 and 1200 °C and idle between 200 and 800 °C. InAlGaAs materials are deposited at a substrate temperature of 500–750 °C. This considerable heat load is largely dissipated by liquid nitrogen (LN_2) flowing through the cryoshroud. In typical MBE growth, inorganic semiconductors are deposited under the cleanest possible conditions in order to maximize device performance. In contrast, typical OLED materials evaporate between 150 and 450 °C and form nearly amorphous films which can be deposited onto unheated substrates. In addition, the physics governing organic EL is much less sensitive to impurity incorporation during device deposition.[2] Taking these facts into account, we replaced LN_2 with water circulated by a closed cycle chiller. When the cryoshroud is filled with 20 °C water, we obtain an ultimate OMBD base pressure of 2×10^{-10} Torr with the cold effusion cells versus 5×10^{-11} Torr attainable with LN_2. An OMBD pressure of 5×10^{-9} Torr can be maintained during deposition. These vacuum levels have proved to be sufficient for the deposition of state-of-the-art OLEDs.

When the OMBD is vented for service with dry nitrogen, the chiller is reset to run heated water (35–40 °C) through the cryoshroud to inhibit gas condensation on the inner walls of the OMBD. This convenience noticeably improves the OMBD pumpdown time. We have never baked our OMBD system because typical MBE bakeout temperatures approach the sublimation temperatures of some of our organic materials. Although a lower temperature bake might improve our pumpdown time further, our experience indicates that the OMBD background pressure is not as important as other factors, e.g., organic source purity.

Several changes in the *in situ* sample diagnostics were also useful. Because most organic EL materials typically deposit as nearly amorphous films, the RHEED system is not used. Instead, the port occupied by the RHEED electron gun proved to be ideally positioned for the installation of a retractable quartz crystal thickness monitor. Quartz crystal monitors are useful for OMBD flux measurement because conventional post-growth calibration techniques used for semiconductor crystals, such as scanning electron microscopy or surface profilometry, are complicated by the extreme softness of the organic films and the thin organic device layer thicknesses used. Flux measurement during growth is also desirable due to instabilities, which we have observed in the deposition of the organic materials described below. The flange opposite the quartz crystal monitor was replaced by a view port, which permits the OMBD operator to view the position of the quartz crystal monitor, main shutter, and sample holder. In addition, the crystal is protected by an integrated pneumatic shutter, which shields the crystal from stray flux when it is not being used, thereby extending its lifetime.

III. GROWTH-RATE CALIBRATION

We routinely use the quartz crystal monitor for *in situ* thickness measurements. The density setting on the quartz crystal monitor for all of our organic materials is 1.5 g/cm^3. The use of a quartz crystal monitor for growth-rate measurement is complicated by the varying incidence angles of the eight effusion cell ports (depicted schematically in Fig. 2). Precise calibrations were obtained by stabilizing the fluxes with respect to the quartz monitor and measuring the resulting thicknesses *ex situ* with a surface profilometer to obtain the actual growth rate. A correction factor for each source material is then entered as a tooling factor in the crystal monitor controller. When performing profilometry on organic films it is important to use a minimal stylus pressure to minimize errors from the stylus digging into the organic layer. We typically coat the organic layer with an Al cap of known thickness to improve the accuracy of the profilometry by presenting a harder surface to the stylus, and then subtracting the Al thickness from the resulting measurement.

Our typical OMBD deposition rates are 0.1 to 0.3 nm/s, which are about the same as those used for GaAs MBE. However, owing to the much shorter mean free paths and lower mobilities of charge carriers in organic materials compared to crystalline inorganic semiconductors, OLED device layers are $\approx 20\times$ thinner ($\approx$50 nm) than typical semiconductor layers ($\approx$1 μm). An OLED deposition run can therefore be completed in 30 min or less, compared to the several hours typical of MBE. The OMBD growth rate influences the morphology of the organic films, particularly the degree of crystallinity, and should therefore be optimized for each organic material and OLED structure.[5]

The sample manipulator depicted in Fig. 3 includes a heater and an ion flux gauge, which are crucial for GaAs epitaxy, but unnecessary or even deleterious during OMBD operation. For example, because of the low glass-transition temperatures of some organic EL materials, if the substrate is heated during or after deposition these materials crystallize, leading to device failure. Thus the heater is generally not used during deposition. It may be desirable in future OMBD designs to integrate a heater controllable at much lower temperatures than typically used in GaAs MBE. The ability to control the substrate temperature accurately up to only 150 °C, for example, might be useful as an additional parameter for the manipulation of film morphology and device performance.[6]

The ion flux gauge is used in semiconductor MBE to measure directly As_4 or As_2 beam equivalent pressures in the 10^{-4}–10^{-5} Torr regime. However, it is advisable to turn off the flux gauge during GaAs epitaxy because of its tendency to outgas during operation. In the

OMBD, the flux gauge serves as a nice complement to the quartz crystal monitor. It is especially useful for measuring smaller fluxes that cannot be detected by the quartz crystal. For example, the flux gauge is accurate for deposition rates of approximately 0.01 nm/s, which is a typical rate for organic dopants for OLEDs. In another application, Haskal et al.[7] used the OMBD flux gauge to measure and calibrate minuscule Li fluxes for optimizing a Li-doped Al OLED cathode structure. However, the flux gauge generates a significant heat load on the sample manipulator when it is on, causing the sample manipulator thermocouple to measure 80–100 °C. The pressure in the OMBD chamber is also adversely affected by outgassing related to ion flux gauge use; first from the flux gauge filament, and then by the increasingly warm sample manipulator. As the quartz crystal monitor is sufficiently accurate and more convenient for routine growths, our flux gauge is used only for measuring and calibrating tiny fluxes, and then only as long as possible before actual OLED deposition.

IV. SAMPLE TRANSFER SYSTEM

A major advantage of adapting a commercial MBE system for OLED use is that it already contains a sample transfer mechanism. To meet OLED fabrication requirements, we designed a shadow masking system on top of the existing sample transfer mechanism. Shadow masking is necessary because conventional semiconductor patterning and etching procedures are incompatible with our vacuum-evaporated OLED materials and, in addition, shadow masks permit OLED fabrication to be completed within the OMBD without exposing the samples to air.

Figure 4 is a schematic of a typical OLED device structure showing the various shadow mask steps required. Typically, we use a Corning 7059 glass substrate with a patterned set of e-beam evaporated or sputtered ITO anode and cathode contact pads. Our ITO/glass substrates incorporate four distinct but identical devices. Use of high-quality glass is important because normal float glass can introduce impurities, especially Na, into the devices. The organic layers are deposited through a shadow mask, which permits uniform organic deposition across the entire device region, but blocks deposition near the edges of the substrate, thereby keeping the ITO contact pads clean. The metal cathode, whose overlap with the ITO anode defines the device area, is deposited through another shadow mask. The design of the organic layer shadow mask also ensures that the cathode makes electrical contact to the ITO cathode contact pad near the substrate edge. In this example, two shadow masks together with pre-patterned ITO are required for *in situ* device fabrication. More complicated masking schemes can also be employed; for example, it is highly desirable to fabricate side-by-side devices on the same substrate using shared process steps for all but one parameter. Such a procedure permits us to assess quickly and accurately the importance of a particular process parameter.

Figure 5 is a photograph of our OMBD substrate holder, which is compatible with both the MBE transfer system and our own shadow-masking design. As substrate heating is not used, thermal contact between the holder and substrate is not an issue and a mechanical method can be used to mount the substrate on the holder. Our patterned, 50±0.1-mm square ITO/glass substrates fit neatly into the two raised right angles seen at the two lower corners of the substrate. The right angles ensure that the substrate is positioned precisely with respect to the shadow masks. The substrate is secured by one or more spring clips, which are tightened by a single screw anchored in a tapped hole.

Our substrate holders use the Varian Gen II MBE outer ring section, which contains three adjacent pairs of asymmetric "figure-8" holes. Figure 6 is a diagram of one pair of adjacent figure-8 holes, which illustrates how the substrate holder can be removed from the carriage.

Cone-tipped posts are inserted through the larger side of one figure-8 until the post's smaller diameter section is in the plane of the holes. A clockwise rotation moves the post into the smaller diameter hole. Once the post is in the smaller diameter hole, the cone shape ensures that the post can no longer move in and out with respect to the sample holder. Further clockwise rotation turns the sample until the opposing post rests in the larger-diameter hole of the adjacent figure-8. At this point, the sample has been transferred from one set of posts to the other.

This sample transfer concept was adapted for our shadow mask design. In the inner section of the sample holder shown in Fig. 5, three posts can be seen extending upwards from the interior of the sample holder. These posts have the same conical design illustrated in Fig. 6. Figure 7 is a photograph of a shadow mask secured to the substrate holder from Fig. 5. Shadow masks are manipulated using the outer sets of figure-8 holes, but secured to the substrate holder using the inner three figure-8 holes.

One important aspect of this design are the sheet metal springs associated with each shadow-mask-securing post. The metal springs are designed such that the shadow mask depresses them when it is mounted on the sample holder. The depressed metal pieces provide an upward pressure on the shadow mask against the larger-diameter top section of the posts, which ensures that the mask is aligned parallel to the substrate and is not free to rotate once mounted. Figure 8 is a schematic illustration of the sheet metal spring pushing against the shadow mask.

We have successfully used up to five different shadow masks in a single run to define features as small as 1 mm. For the sharpest possible features, the shadow mask should be thin and as close as possible to the sample surface. Our shadow masking system permits us to prepare side-by-side devices on a single substrate where only one anode, cathode, or organic layer parameter has been varied between devices.

V. OMBD SOURCE MATERIALS AND OPERATION

Five effusion cells are typically used for the fabrication of our standard OLEDs. Three cells each contain one member of our standard organic materials set: CuPc, NPB or Alq_3.[8] Two other cells contain the cathode metals Al and Ca (or alternatively Ag and Mg, or Al and Li). The remaining three ports are used for various other organic materials, as well as experimental electrode materials. We have discovered that nearly all of the materials used in OMBD require special considerations that are not obvious to an experienced GaAs MBE practitioner.

These organic materials sublime in the temperature range of 150–450 °C. As we received conventional GaAs type-C thermocouple effusion cells with pyrolytic boron nitride (PBN) crucibles along with the MBE system, we were concerned whether these cells would be stable at low temperatures. Inorganic semiconductor MBE users working with II–VI materials have previously faced this issue with Hg. To address these concerns we purchased type-K thermocouples in low-temperature effusion cells. In retrospect, the low-temperature cells were unnecessary for our organic sources, with the possible exception of organic dopant materials whose fluxes must be controlled at much lower levels and within tighter specifications. We have observed no flux instabilities related to the type-C effusion cells when organic compounds are evaporated at temperatures below 300 °C.

PBN crucibles are engineered for cleanliness at extremely high temperatures, but are quite expensive. We have found that quartz is an entirely adequate and significantly cheaper substitute for use in organic effusion cells. However, we still use PBN crucibles for the inorganic materials, most of which are evaporated at the much higher temperatures typical in MBE.

All of the organic materials used in the OMBD are commercially available, although the purity of the materials varies from vendor to vendor. It is therefore standard procedure in our laboratory to purify all organic materials at least once using a gradient sublimation technique.[9] Typically, the organic compound is heated to its sublimation temperature in an evacuated horizontal quartz tube situated within a multizone furnace. In this configuration, volatile contaminants evaporate quickly and are pumped out of the chamber. When the temperature is raised slowly, organic components evaporate and recondense in the cooler regions of the temperature gradient set across the quartz tube. Purified organic material can then be removed by scraping the proper region of the quartz tube in a clean environment, whereas impurities left behind or condensed in other areas can be discarded. The initial purity of the material can be estimated by the overall yield of the purification cycle and by the amount of initial outgassing. This information is used to decide whether additional purification cycles are necessary, and partly to select among competing materials vendors. Some organic material is sufficiently pure that we see no improvement in OLED performance when we purify the material after delivery. Other materials require only a simplified vacuum purification onto a cooled deposition surface in a single-zone furnace. Inorganic materials are available in sufficiently high purity that they can be loaded immediately into the OMBD.

As only four effusion cell flanges are tilted upwards, some effusion cells must be mounted in downward-facing flanges, so we needed to develop methods to avoid material loss simply due to gravity. We routinely sublime Ca, CuPc, and Alq_3 from effusion cells in the downward-facing flanges. To solve this problem, MBE practitioners have previously used an inverted two-crucible scheme in which an inner crucible is tilted upwards within an outer crucible facing downwards. We developed a simpler solution, which was facilitated by the nature of the materials we chose to evaporate from the upper ports and their low evaporation temperatures.

Calcium lends itself well to a downward-facing cell. It evaporates like As, becoming more porous as it is depleted while its volume remains largely unchanged. Because clean Ca source material is sticky, it is possible to fill the PBN crucible with closely packed material that does not fall out when the effusion cell is loaded in a downward-facing OMBD flange, and the Ca charge remains stable during evaporation.

As the organic materials we used are powdery, it was impossible to adopt this approach. Instead we attached a doughnut-shaped Ta foil to the open end of our crucibles to act as a dam against material loss. This has the effect of reducing the cell aperture diameter to $\approx$1 cm, but the foil barrier blocks Alq_3 or CuPc powder from sliding out of the crucible. Sample uniformity did not suffer as a result of the reduced cell aperture. Using this configuration, we found that growth of Alq_3 was the most reproducible of all of our OMBD source materials.

In the case of CuPc, an unexpected but eventually benign (or even favorable) phenomenon was observed when we mounted the source downward with a doughnut-shaped Ta foil aperture. This phenomenon is depicted in Fig. 9, where the CuPc effusion cell thermocouple reading corresponding to constant flux conditions is plotted against successive OMBD runs immediately following the installation of fresh CuPc source material. The temperature required for constant CuPc flux is stable over the initial few runs, and then increases sharply over the next several runs until it saturates at a higher temperature. After saturation, the run-to-run CuPc flux-temperature relationship is extremely stable for as long as the CuPc source remains undisturbed and the source material undepleted.

When we removed the CuPc source before it became depleted, we observed that CuPc had clogged the aperture at the mouth of the cell. We believe that the increase in the effusion cell temperature required for constant flux initially reflects the decreasing aperture size through which CuPc can exit the crucible. Later, once the aperture has become completely clogged, a higher operating power is required to heat the CuPc plug to its sublimation temperature owing to increased radiative losses at the mouth of the cell. A beneficial effect of this entire process may be that the CuPc charge undergoes an additional purification during the transfer of material from the back of the crucible forward to the foil aperture in a process quite similar to our gradient sublimation purification technique.

We have also observed clogging in our NPB effusion cell when an aperture is installed. However, in contrast to CuPc, NPB clotting is undesirable because it leads to flux bursts and irregular flux-temperature behavior. The NPB source is always mounted in an upward-facing effusion cell port because the sublimation temperature corresponding to the typical growth rate is near the NPB melting point. As with CuPc, the constant-flux thermocouple reading was observed to rise with consecutive OMBD runs. When the aperture became blocked, the effusion cell could be reproducibly operated only at a much lower NPB flux than desired. At this point the working temperature was set at $\approx$50 °C higher than the initial thermocouple temperature. Further increasing the effusion cell power precipitated an NPB burst at an extremely high level ($\approx$2.5 nm/s), after which the flux–temperature relationship was restored to the initial curve observed before clotting. Our interpretation is that at higher temperatures, the NPB plug reached its melting point where it contacted the Ta foil aperture, thereby causing the plug to fall back into the crucible, where it melted immediately. Operating the NPB cell in this manner wasted significant amounts of material, and also required excessive vigilance on the part of the operator, as it provided too little flux as the aperture became clogged and much too high a flux after the plug was cleared. The problem was easily solved by loading NPB into a crucible with a much wider mouth and eschewing the use of any Ta foil aperture.

Metal sources in OMBD behave much like in conventional GaAs MBE, and therefore present few obvious problems for OMBD. As with MBE, care must be taken to avoid cracking PBN crucibles by rapidly freezing liquid metal charges, most notably Al, but also Ag. To avoid the deposition of organics near the metal cells, we idled the metal sources at high temperature (850 °C for Al). This has the added advantage of maintaining the Al charge above its freezing point to reduce the chance of the PBN cracking after numerous melt/freeze cycles.

A second problem is radiative heating of the substrate during metal deposition. This is illustrated by the fact that when the Al shutter is open, the substrate is bathed in red light emanating from the hot (>1000 °C) Al charge and effusion cell. We observed that OLEDs exposed too long to the Al cell exhibited evidence of recrystallization, indicating that the device had been heated above the glass transition temperature of one or more of the organic compounds. An adequate solution to this problem was to pull the hotter effusion cells back by inserting an extender nipple between the source flange effusion cell port and the effusion cell. The Al cell, which we retracted 8", is visible in Fig. 1 (the lowest of the three visible effusion cells). Upon inserting the extender nipple, we no longer observed organic layer recrystallization following Al deposition.

A third issue related to the metal sources in the OMBD is undesired contamination of the organic layers during growth. We observed that if either Al or Ca is at deposition temperature with the effusion cell shutter closed while organic layers are being deposited, the performance of the OLEDs was greatly degraded. This effect could be due to either contamination of the OLED from outgassing in areas heated by the metal effusion cell, or by metal flux escaping around the shutter and finding its way into the growing film. Regardless of the cause, the solution is to maintain the metal cells at their lower idling temperatures during organic film depositions.

Generally we idle all effusion cells at an elevated temperature to avoid condensation of water vapor or volatile organics in or near the source material. Because of the low sublimation temperatures, we idle organic sources such as NPB and Alq_3 at 100 °C. CuPc is idled at 200 °C because the effusion cell thermocouple does not correspond to the actual temperature of the clotted material within the Ta aperture. Al and Ag idle above their melting points, and Ca is idled at 200 °C, as are whatever other inorganic sources being used.

We have implemented computer control of the OMBD sources and their shutters by adapting LabView software.[10] Computer control permits us to complete an entire OLED deposition procedure automatically and reproducibly, with the exception of sample transfer and shadow mask changes. Another program permits the Al cell to be ramped slowly through its freezing point to avoid cracking the PBN crucible when cooling it to room temperature for service. In an OMBD production environment incorporating high-volume, stable effusion cells, computer control is very convenient. In our research environment, in which we vary our deposition parameters and materials often and must still change shadow masks manually, computer control saves less time, and the OMBD is usually controlled directly by the operator for the 1 h or less required to deposit an OLED with multiple masks.

VI. SUMMARY

We have described the conversion, installation, and operating procedures of the OMBD system. Using these procedures in the above-described system, we consistently produce OLEDs comparable to state-of-the-art published results, which were obtained using the same organic materials set. We are therefore confident that our design and procedures will assist future workers in converting or designing a vacuum system for OMBD.

ACKNOWLEDGMENTS

The authors are grateful to the members of the IBM Zurich machine shop, and to T. Beierlein, H. P. Meier, and A. Witzig, for their assistance with the transport, design, conversion, and operation of the OMBD.

[1] C. Tang and S. A. Van Slyke, Appl. Phys. Lett. **51**, 913 (1987).
[2] S. Strite and W. Riess, Compound Semiconductor Magazine **3/6**, 35 (1997).
[3] S. V. Iyer, H. P. Meier, S. Ovadia, C. Parks, D. H. Arent, and W. Walter, Appl. Phys. Lett. **60**, 416 (1992).
[4] C. C. Wu, C. I. Wu, J. C. Sturm, and A. Kahn, Appl. Phys. Lett. **70**, 1348 (1997).
[5] M. Komiyama, Y. Sakakibara, and H. Hirai, Thin Solid Films **151**, L109 (1987).
[6] H. Masui and M. Takeuchi, Jpn. J. Appl. Phys. **30**, L864 (1991).
[7] E. I. Haskal, A. Curioni, P. F. Seidler, and W. Andreoni, Appl. Phys. Lett. **71**, 1151 (1997).
[8] C. Tang, Information Display **12/10**, 16 (1996).
[9] S. R. Forrest, P. E. Burrows, E. I. Haskal, and F. F. So, Phys. Rev. B **49**, 11309 (1994).
[10] National Instruments Corporation, Austin, TX.

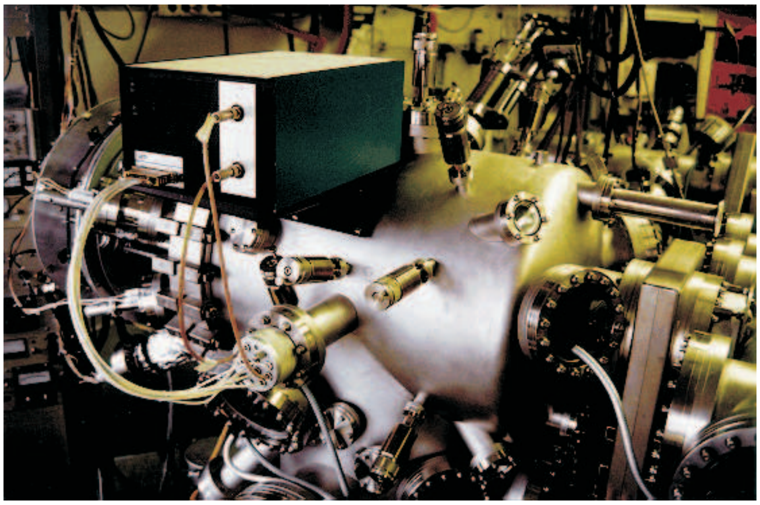

FIG. 1. Organic molecular beam deposition system at the IBM Zurich Research Laboratory.

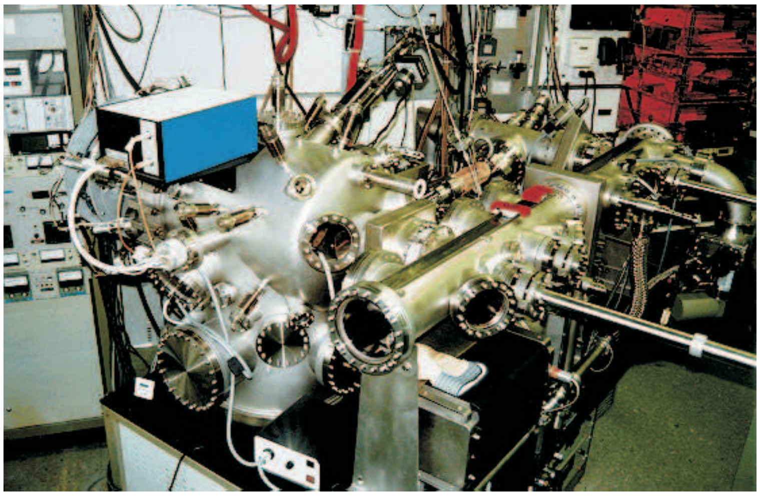

FIG. 2. Complete vacuum system showing the OMBD chamber, the rf-plasma processing chamber, load lock, and transfer chamber. Samples can be transferred between the various chambers without breaking vacuum, permitting experiments of greater complexity and variety than are possible in a single OMBD chamber.

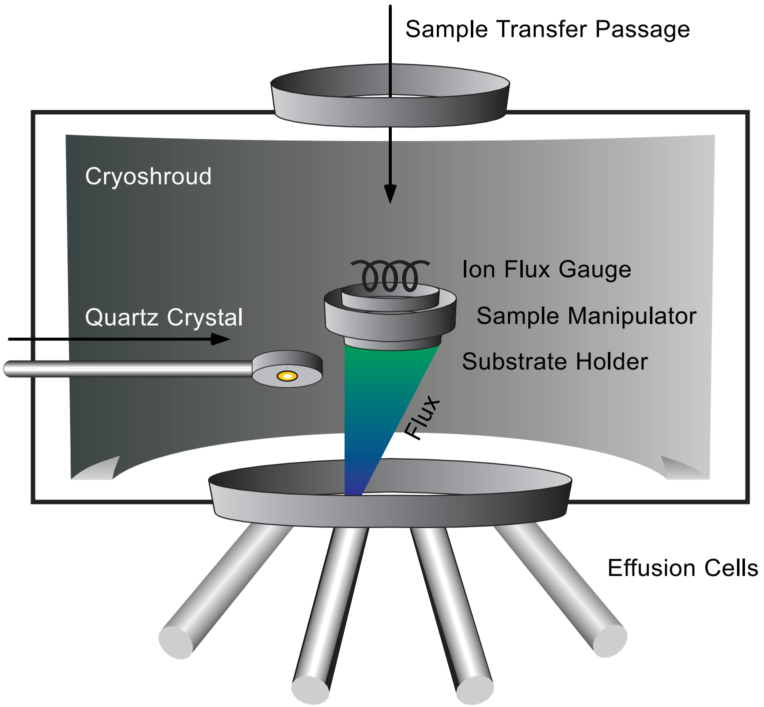

FIG. 3. Schematic of the OMBD system. Major alterations of the original MBE chamber include the replacement of liquid nitrogen in the cryoshroud with chilled water and the installation of a quartz crystal deposition monitor on a retractable bellows.

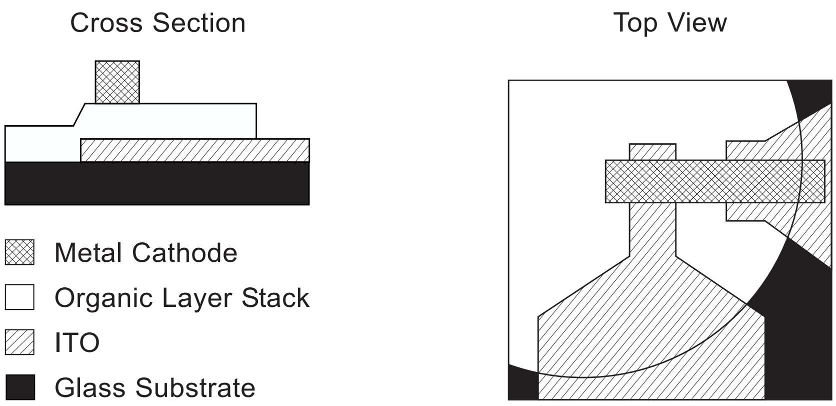

FIG. 4. Diagrams illustrating the shadow masking used for different device layers. The simple OLED structure shown here requires a mask for the organic materials, a mask for the top cathode, and pre-patterned ITO.

FIG. 5. Photograph of an OMBD sample holder with an ITO/glass substrate mounted on top. The substrate is held in place by two raised right angles and one or more clips.

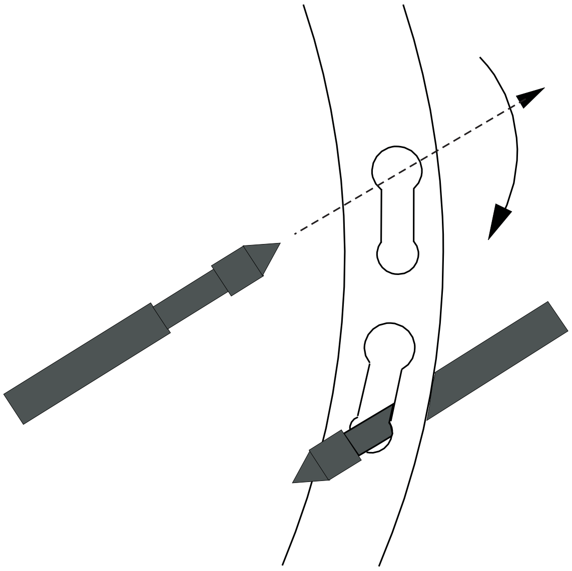

FIG. 6. Diagram of the transfer mechanism. Magnified view of an outer ring section of the substrate holder illustrates the action of removing the substrate holder from a fixed position, e.g., the OMBD sample manipulator. To transfer a sample holder, a set of three posts is guided into the holes, and then rotated to lock the posts into position.

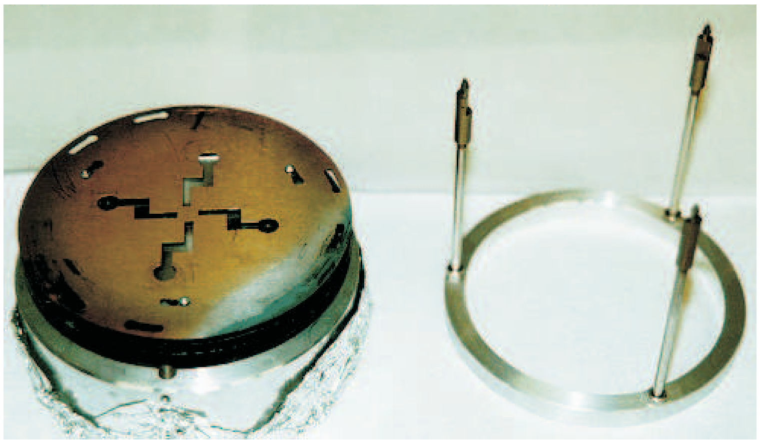

FIG. 7. OMBD sample holder with a secured shadow mask.

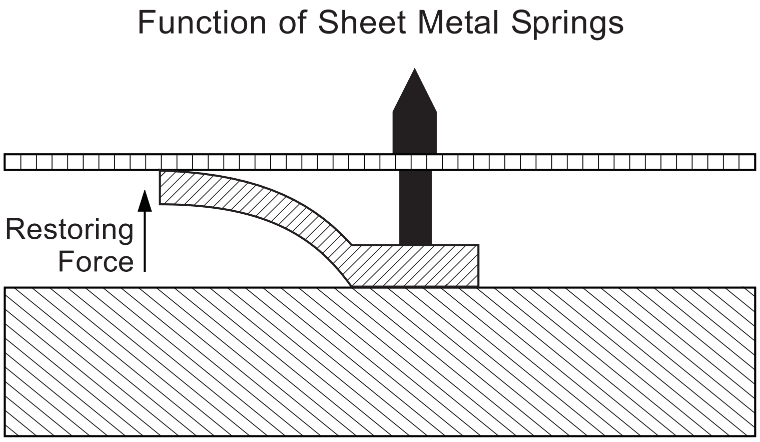

FIG. 8. Schematic of the function of the sheet metal springs used to secure the shadow mask parallel to the substrate holder.

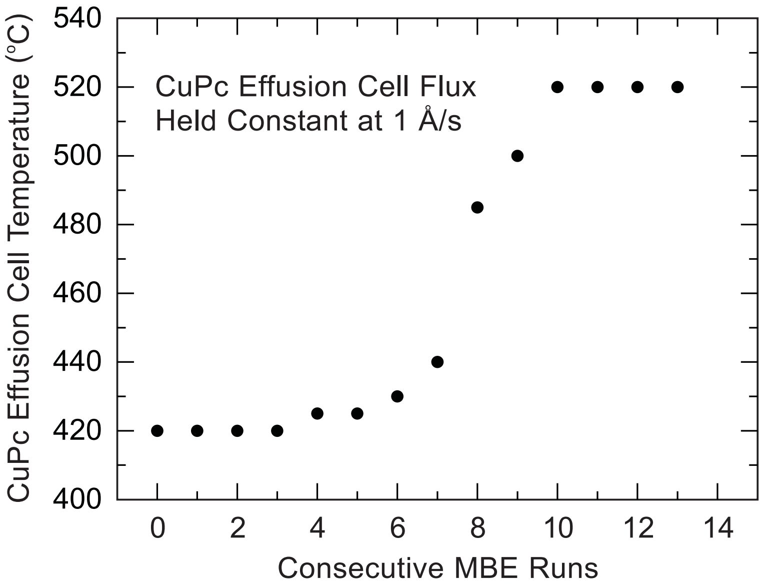

FIG. 9. Behavior of the CuPc effusion cell in consecutive runs. Clogging of the aperture occurs because of a redistribution of the CuPc from the back to the mouth of the crucible. During the clogging process, higher temperatures were required to maintain constant flux as a result of the reduced aperture size. By the tenth run, the aperture was fully clogged and the flux-temperature relationship became constant.